

Assessment of isoconversional methods and peak functions for the kinetic analysis of thermogravimetric data and its application to degradation processes of organic phase change materials

Rocío Bayón¹ ○ · Redlich García-Rojas¹ · Esther Rojas¹ · Margarita M. Rodríguez-García¹

Received: 17 October 2023 / Accepted: 9 July 2024 / Published online: 3 October 2024 © The Author(s) 2024

Abstract

In this work, theoretical kinetic curves of both single- and multi-step reaction mechanisms were simulated by using different sets of kinetic parameters. Various isoconversional methods were applied for the kinetic analysis of these curves so that the corresponding activation energy vs. conversion degree curves were obtained and then compared with the energy values used in the simulations. For single-step reaction mechanisms Friedman method resulted to be the most accurate while for multi-step reaction mechanisms, Kissinger-Akahira-Sunose and Coats-Redfern methods led to the most accurate estimation of the activation energy. On the other hand, conversion rate curves of different single-step reaction mechanisms were fitted with two kinds of peak functions (normalized Fraser-Suzuki and generalized logistic) so that the relationships between the parameters of these functions and the kinetic parameters used in the simulations were obtained. These relationships were then used in the mathematical deconvolution analysis of conversion rate curves simulated for multi-step reaction mechanisms. In general, the curves resulting from deconvolution fitted quite well the simulated conversion rate curves and the analysis of the resulting single-step reaction curves with Kissinger method led the kinetic parameters close to the ones used in the simulations. Finally, a similar kinetic analysis was applied to experimental thermogravimetric measurements taken both under N₂ and air for two phase change materials (PCMs) based on polyethylene glycol, PEG6000 and PEG12000. Activation energy values obtained with isoconversional methods for the measurements under N₂, varied from 40 kJ mol⁻¹ at low conversions up to 150 kJ mol⁻¹ at high conversions, whereas for the measurements under air the energy values remained almost constant in the range of 50-75 kJ mol⁻¹. The lower activation energies obtained for the measurements under air are clearly associated with the polymer combustion. The experimental conversion rate curves were deconvoluted with the most appropriate peak functions so that the possible single-step reaction mechanisms occurring in these PCMs were separated and further analyzed with Kissinger method. The activation energies obtained with this method were in good agreement with the values resulting from the isoconversional methods.

 $\textbf{Keywords} \ \ Kinetic \ analysis \cdot Isoconversional \ methods \cdot Fraser-Suzuki \ function \cdot Generalized \ logistic \ function \cdot Fitting \cdot Mathematical \ deconvolution \ analysis \cdot TG \ measurements \cdot PCM$

Abbreviations		dTA	Differential thermal analysis
A	Frequency factor or pre-exponential factor	FWO	Flynn-Wall-Ozawa
	in s^{-1}	GLOG	Generalized logistic probability density
E	Activation energy in kJ mol ⁻¹		function
CR	Coats-Redfern	KAS	Kissinger-Akahira-Sunose
dTG-T curve	Conversion rate and also derivative of the	MDA	Mathematical deconvolution analysis
	thermogravimetric curve	NFS	Normalized Fraser-Suzuki function
		PCM	Phase change material
		PEG	Polyethylene glycol
⊠ Rocío Bayón rocio.bayon@ciemat.es		TG curve	Thermogravimetric curve
		α	Conversion degree $\frac{m_{\rm ini}-m}{m_{\rm ini}}$

Thermal Energy Storage Unit, CIEMAT-PSA, Av. Complutense 40, 28040 Madrid, Spain



 α -T curve Conversion degree variation with temperature

Heating rate used in the thermogravimetric

measurement in $K \min^{-1}$

Introduction

β

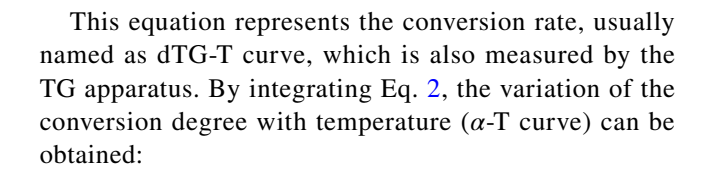
Phase change materials (PCMs) with melting temperatures (T_m) between 30 and 160 °C are of particular interest for thermal energy storage applications in both low- and midtemperature ranges. In terms of practical implementation, one of the most critical issues when choosing a PCM for a certain application is to be sure that the material keeps its performance along the whole service life of the storage system. In most references found in the literature, PCM long-term performance is assessed through melting/freezing cycles or just by analyzing thermogravimetric (TG) curves (i.e., mass loss over temperature) measured at only one heating rate. However, if the material suffers some kind of degradation after melting, cycles may lead to misleading results because such degradation will be hindered during the freezing period. On the other hand, the information obtained from TG curves in terms of temperature limit for material stability strongly depends on the heating rate used in the experiment. Hence, these tests are not sufficient for validating either the stability nor the successful life performance of a PCM. Therefore, for assessing the long-term stability of PCM, the starting point is to carry out a kinetic analysis of the TG measurements in order to determine the possible degradation processes [1, 2].

The majority of kinetic methods used in the area of thermal analysis consider the reaction rate equation [3]:

$$\frac{\mathrm{d}\alpha}{\mathrm{d}t} = k(T)f(\alpha) = A\mathrm{e}^{\left(\frac{E}{RT}\right)}f(\alpha) \tag{1}$$

which is a function of only two variables: temperature, T, and conversion degree, $\alpha = \frac{m_{\rm ini}-m}{m_{\rm ini}}$. The dependence of the process rate on temperature is represented by the rate constant, k(T) which is typically parameterized through the Arrhenius equation in which A is the so-called frequency or pre-exponential factor, E is the activation energy and R is the molar gas constant. The dependence on the conversion degree is represented by $f(\alpha)$, which is a function whose formulation depends on the mathematical model describing the reaction mechanism. For the particular case of dynamic TG measurements taken at constant heating rate $\beta = \frac{\mathrm{d}T}{\mathrm{d}t}$, Eq. 1 becomes:

$$\frac{\mathrm{d}\alpha}{\mathrm{d}T} = \frac{Af(\alpha)\mathrm{e}^{-\mathrm{E/RT}}}{\beta} \tag{2}$$



$$\int_{0}^{\alpha} \frac{d\alpha}{f(\alpha)} = g(\alpha) = \frac{A}{\beta} \int_{T_{0}}^{T} e^{-E/RT} dT$$
(3)

In this equation, $g(\alpha)$ is a function calculated from $f(\alpha)$ so that it also depends on the model used to describe the reaction mechanism [3]. $\int_{T_0}^T e^{-E/RT} dT$ is the temperature integral [4], which cannot be calculated explicitly so that either numerical methods or analytical approximations have been proposed by different authors for its evaluation [5]. In our case, we have taken the Coats and Redfern approximation for calculating the temperature integral [6].

The aim of any kinetic analysis is to obtain the kinetic triplet: E, A and $f(\alpha)$. If the reaction mechanism $f(\alpha)$ is unknown, the activation energy, E, can be estimated in a first approach by using one or more model-free isoconversional methods that are already described in the literature. These methods can be grouped in differential, if they are based in Eq. 2, or integral, if they are based in Eq. 3 [3]. Among the differential, we have the method of Friedman [7], and among the integral, we have the methods of Coats and Redfern [6], Ozawa [8], Flynn-Wall [9], Akahira and Sunose [10], Kissinger [11], and Miura and Maki [12]. These are what we can call the traditional isoconversional methods; however, there are other methods more sophisticated that are based on numerical integration like the one developed by Vyazovkin [13, 14]. If the reaction takes place in a single-step process, E should not vary significantly with α , and hence, A and $f(\alpha)$ could be obtained by applying some of the methods already stablished by the Kinetics Committee of the International Confederation for Thermal Analysis and Calorimetry (ICTAC) [3, 15]. Examples of these methods are Kissinger [11], Coats–Redfern with discriminating approach [6] or the method based on the so-called master plots [3].

Conversely, for multi-step processes, the E calculated with the isoconversional methods is expected to change with α due to the different relative contributions of each single-step to the overall reaction rate. The occurrence of multi-step processes is also detected if dTG-T curve does not present a unique maximum but it presents various peaks, which may be more or less overlapping. In such case, each reaction step should be separated and analyzed independently [15]. There are several ways to separate overlapping peaks of single-step reactions. The most common one consists in performing a mathematical deconvolution analysis (MDA) by using asymmetric peak functions [15]. However, some authors have proposed alternative methods based in



nonlinear regressions for estimating kinetic parameters of complex multi-step processes [16]. After single-step processes are separated, the kinetic triplet for each reaction could in principle be obtained by applying the different methods mentioned above.

One of the most widely used functions for MDA of dTG-T curves is the one proposed by Fraser and Suzuki (FS) [17, 18]. In fact, there are many examples in the literature that use FS function in the kinetic analysis of thermogravimetric measurements for different kinds of materials undergoing multi-step reactions [19–22]. Some authors have used other peak functions like Gaussian, Lorentzian or Weibull for fitting dTG-T curves [19], but in the end the best fitting was always obtained with the FS curve. There is, however, a peak function that, to our knowledge, has never been used for MDA of dTG-T curves but could represent and advantage over the FS function due to its less restrictive mathematical formulation. This function is the generalized logistic probability density function (GLOG) [23] also known as Richards curve.

In this context, this work had three main objectives: The first one was to assess which isoconversional method is the most adequate for having a preliminary estimation of the activation energy, E, of multi-step reaction process; the second one was to determine which peak function better represents the different reaction mechanisms, i.e., which one fits dTG-T curves more accurately and, the third one, was to find a correlation between the kinetic triplet and the parameters of the fitting functions.

For that purpose, theoretical kinetic curves of conversion degree (α -T) and conversion rate (dTG-T) were constructed for different reaction mechanisms, $f(\alpha)$, known Arrhenius parameters, E and $\ln A$, and various heating rates, β . Also similar sets of curves were simulated for multi-step reaction mechanisms with two parallel single-step independent reactions. Both single-step and multi-step theoretical curves were analyzed by different isoconversional methods in order to obtain the variation of activation energy with the conversion degree $(E-\alpha)$ and determine which method is the most adequate for analyzing real experimental data from TG measurements. Subsequently, the simulated dTG-T curves of single-step reactions were fitted with two peak functions: the normalized Fraser-Suzuki (NFS) and the generalized logistic (GLOG). With this analysis, it would be possible to determine which function is the most appropriate for representing each reaction mechanism and also the relationship between both the function parameters and the kinetic parameters used in the simulations. Additionally, mathematical deconvolution analysis (MDA) was applied to dTG-T curves simulated for multi-step reaction mechanisms so that the single-step reaction curves were separated. The kinetic parameters E and lnA of these single-step reactions were obtained and then compared with the corresponding values used in the simulations.

Finally, the procedure of kinetic analysis developed for the theoretical kinetic curves was applied to the particular case of polyethylene glycol (PEG) with two molecular weights: 6000 and 12000. This PCM was chosen because up to now the kinetics of thermal degradation of polyethylene glycol have not been obtained. In fact, all references found in the literature where its thermal stability is studied establish the temperature interval in which degradation occurs and the temperature at which degradation rate is maximum by analyzing TG measurements taken at only one heating rate [24–28]. Therefore, in order to have a first insight into PEG thermal degradation kinetics, TG measurements were taken for both PEG3000 and PEG 12000 under N2 and air atmospheres at heating rates from 2 to 20 K min⁻¹. These measurements were analyzed by the different isoconversional methods applied in this work so that E- α curves were obtained. Also, mathematical deconvolution analysis was applied to dTG-T curves by using the most appropriate peak functions so that single-step reactions were separated and the corresponding activation energies calculated. Finally, the activation energy values obtained by both procedures were compared and discussed.

Construction of the theoretical kinetic curves

According to the previous literature, the mechanisms of the chemical reactions can be described by specific mathematical expressions for the function $f(\alpha)$ [3]. Šesták–Berggren general equation puts together most of the kinetic mechanisms by using a unique empirical equation with three parameters: m, n and p.

$$f(\alpha) = \alpha^{\mathrm{m}} (1 - \alpha)^{\mathrm{n}} [-\ln(1 - \alpha)]^{\mathrm{p}}$$
(4)

 $f(\alpha)$ function associated with different reaction mechanisms can be obtained by giving specific values to the Šesták–Berggren parameters. In Table 1, the mathematical expressions of both $f(\alpha)$ and $g(\alpha)$ are recorded for the reaction mechanisms whose kinetics have been theoretically simulated in this work.

Using Eqs. 2 and 3, sets of theoretical kinetic curves α -T and dTG-T were simulated for all the mechanisms displayed in Table 1 at the heating rates, β , recorded in Table 2. The values of E and $\ln A$ used in the simulations are also displayed in Table 2, and they were chosen by taking into account the values considered by other authors for constructing similar theoretical curves to carry out kinetic analysis [19, 29–32]. Moreover, according to our previous experience



Table 1 Reaction mechanisms and their corresponding $f(\alpha)$ and $g(\alpha)$ expressions used for simulating the theoretical kinetic curves α -T and dTG-T

Model ID	Reaction mechanism	$f(\alpha)$	$g(\alpha)$
F0	Zero order	1	α
F1	(Mampel) First order	$(1-\alpha)^1$	$-\ln(1-\alpha)$
F2	Second order	$(1-\alpha)^2$	$(1-\alpha)^{-1}-1$
D1	One-dimensional diffusion	$\frac{1}{2\alpha}$	α^2
D3	Three-dimensional diffusion	$[3(1-\alpha)^{2/3}]/[2(1-(1-\alpha)^{1/3})]$	$\left[1 - (1 - \alpha)^{1/3}\right]^2$
Random nuc	leation and instantaneous growth of r	nuclei	,
A1≡F1	Avrami–Erofeev (n=1)	$(1-\alpha)^1$	$-\ln(1-\alpha)$
A2	Avrami–Erofeev (n=2)	$2(1-\alpha)[-\ln(1-\alpha)]^{1/2}$	$[-\ln(1-\alpha)]^{1/2}$
A3	Avrami–Erofeev (n=3)	$3(1-\alpha)[-\ln(1-\alpha)]^{2/3}$	$\left[-\ln(1-\alpha)\right]^{1/3}$
A4	Avrami–Erofeev (n=4)	$4(1-\alpha)[-\ln(1-\alpha)]^{3/4}$	$[-\ln(1-\alpha)]^{1/4}$
R2	Phase boundary controlled (contracting area or cylinder)	$2(1-\alpha)^{1/2}$	$1-(1-\alpha)^{1/2}$
R3	Phase boundary controlled (contracting volume or sphere)	$3(1-\alpha)^{2/3}$	$1-(1-\alpha)^{1/3}$
P2	Power law	$2\alpha^{1/2}$	$\alpha^{1/2}$

Table 2 Kinetic parameters used in the simulation of α -T and dTG-T curves

E/kJ mol ⁻¹	lnA/s ⁻¹	β/K min ⁻¹
60	10, 12	2, 5, 10, 20
80	15, 17, 18, 19	2, 5, 10, 20
90	18, 19	2, 5, 10, 20
100	20, 25	2, 5, 10, 20
120	25, 30	2, 5, 10, 20

in kinetic analysis of TG measurements of various PCMs [2, 33], the values of *E* and ln*A* of Table 2 selected for the theoretical simulations are in good agreement with the ones experimentally obtained.

The shape of simulated α -T and dTG-T curves depended on the reaction mechanism and hence on the associated function $f(\alpha)$ being the differences more clearly observed in dTG-T curves (i.e., peak curves). In this sense, mechanisms F1, A2, A3 and A4 led to quite symmetric curves, mechanisms R2, R3, F2 and D3 led to curves with higher asymmetry, whereas mechanisms F0, D1 and P2 led to spikelike curves. In Fig. 1, simulated dTG-T curves for the heating rates recorded in Table 2 are displayed for the reaction mechanisms A2 (a), R2 (b) and D1 (c), each one representing an example of curve shape. The values of E and lnA used in the simulations are displayed in each graph. The curves simulated for the other reaction mechanisms included in Table 1 are shown in Fig. S1 of the supplementary material. It is important to mention here that not all combinations of E and lnA were used for simulating all mechanisms since the effect of these parameters on dTG-T curves is only the temperature interval they cover. This is clearly shown in Fig. 1 (d), where

curves simulated with $\beta = 2$ K min⁻¹ and different values of E and $\ln A$ are displayed. In Fig. S1 of supplementary material, further examples of this effect can be found for various reaction mechanisms.

Following a procedure similar to the one used by Granado [29] and Sbirrazzouli [32], kinetic curves (α -T and dTG-T) were simulated for multi-step reaction mechanisms with two parallel independent reactions whose overall reaction rate can be expressed as:

$$\frac{d\alpha}{dt} = x_1 A_1 e^{\left(\frac{-E_1}{RT}\right)} f_1(\alpha_1) + x_2 A_2 e^{\left(\frac{-E_2}{RT}\right)} f_2(\alpha_2)$$
 (5)

with $\alpha = \alpha_1 + \alpha_2$ and $x_1 + x_2 = 1$

Combinations of two reaction mechanisms with different kinetic parameters were simulated including one of the cases already studied by Sbirrazzouli [32] (CASE 7). The combination of mechanisms with their corresponding kinetic parameters is given in Table 3.

In Fig. 2, both $(1-\alpha)$ -T (a) and dTG-T (b) curves calculated at 2 K min⁻¹ are displayed for each combination CASE. In Fig. 2a, we can see how $(1-\alpha)$ -T curves of CASES 1, 2 and 6 clearly show one step at the α value that corresponds to the contribution fraction of each single-step reaction. However, $(1-\alpha)$ -T curves of CASES 3, 4 and 5 do not show any clear step, which means that both mechanisms are highly overlapping. This behavior is also observed in dTG-T curves of Fig. 2b; while CASES 1, 2 and 6 show two peaks clearly separated and quite independent, the curves of CASES 3, 4, 5 and 7 present overlapping peaks.



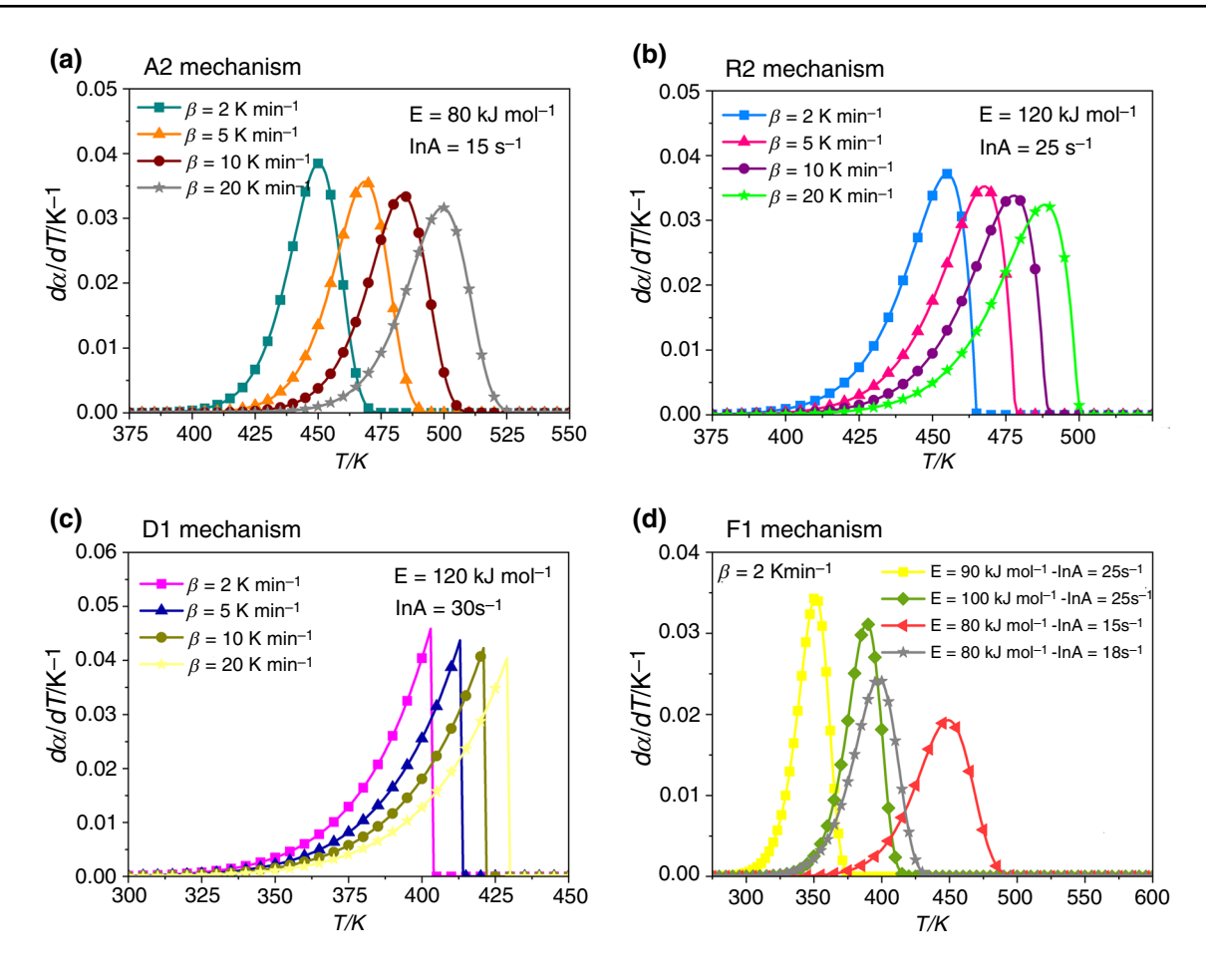


Fig. 1 Examples of dTG-T curves simulated for different reaction mechanisms $f(\alpha)$: A2 (a), R2 (b), D1 (c) and effect of the kinetic parameters E and lnA in dTG-T curve of 2 K min.⁻¹ for the mechanism F1 (d)

Table 3 Kinetic parameters of single-step reactions 2 and 2 used for simulating the multi-step reaction mechanisms of Eq. 5

	Mechanism	E _{1, 2} /kJ mol ⁻¹	lnA _{1, 2} /s ⁻¹	x _{1, 2}
CASE 1	F1	80	18	0.5
	A2	100	20	0.5
CASE 2	F1	80	17	0.8
	A2	100	20	0.2
CASE 3	F1	80	17	0.5
	A2	90	18	0.5
CASE 4	F2	60	15	0.5
	R3	120	30	0.5
CASE 5	F2	60	15	0.2
	R3	120	30	0.8
CASE 6	D3	80	18	0.5
	P2	120	25	0.5
CASE 7 [32]	F1	80	19	0.5
	F1	90	19	0.5

As example, Fig. 3 shows the evolution of dTG-T curves with heating rate, β , for CASE 1, with slight peak overlapping (a) and CASE 3 (b) with strong peak overlapping.

Model-free isoconversional methods for the analysis of single- and multi-step reaction mechanisms

Model-free isoconversional methods allow the activation energy to be estimated as a function of conversion without choosing any reaction mechanism. The basic assumption of these methods is that the reaction rate at constant conversion degree, α , depends only on temperature so that constant E values can be expected [3]. However, if multi-step processes occur, E varies with α due to the different relative contributions of each single-step to the overall reaction rate and also to the fact that those reactions can take place either in parallel or in consecutive form. For this reason, the results from the isoconversional methods may not be fully accurate, but still can serve as a preliminary estimation and, of course, for



checking whether a reaction is composed by one or various single-step processes [15]. The traditional isoconversional methods are based on linear plots with 1/T in the abscissa axis when the same conversion degree occurs. This is done for TG measurements taken at different heating velocities, and the corresponding activation energy is usually obtained from the slope of the linear plot. Table 4 summarizes the

mathematical expressions of the isoconversional methods applied in this work for analyzing the simulated kinetic curves [6, 7, 9, 10].

These four methods were implemented in a self-developed MATLAB© code for automatic calculation. The code allows obtaining E- α curves for each of the four methods recorded in Table 4 and also the intercepts of both Friedman

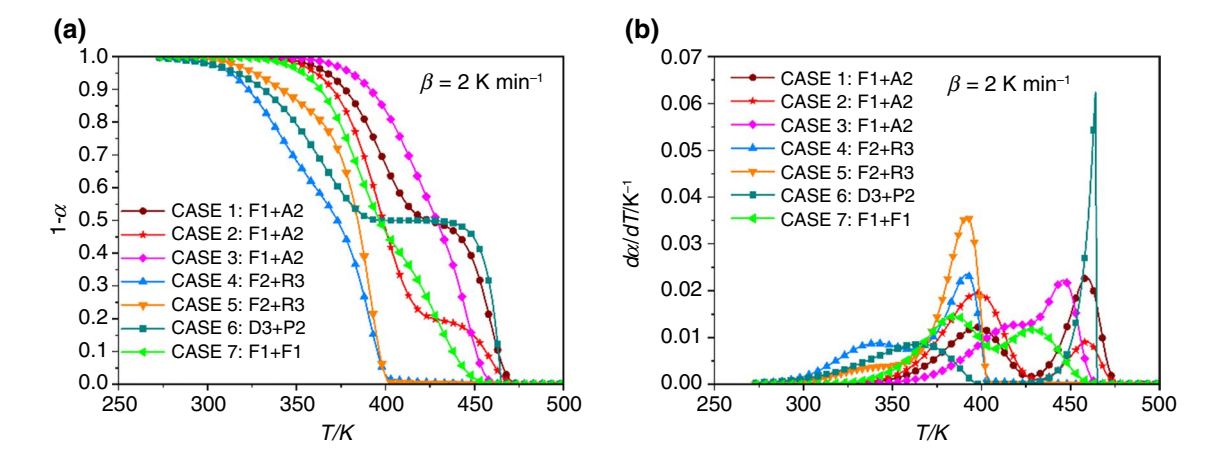


Fig. 2 $(1-\alpha)$ -T (a) and dTG-T (b) curves simulated for CASES 1–7 that combine two single-step reaction mechanisms (see Table 3 for kinetic parameters details)

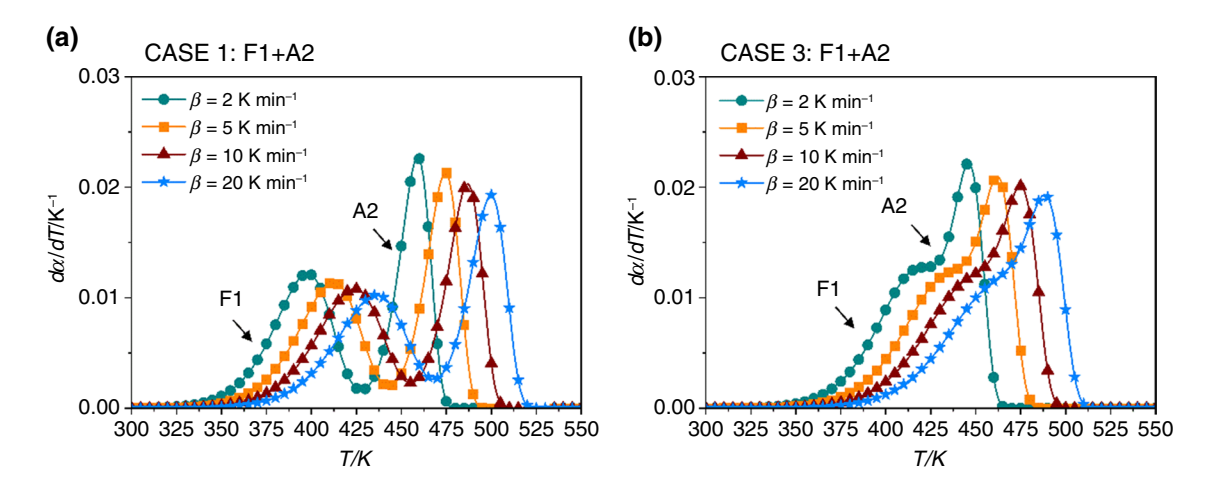


Fig. 3 Evolution of dTG-T curves with heating rate, β , for simulated for CASE 1 with slight peak overlapping (a) and CASE 3 (b) with strong peak overlapping (see Table 3 for kinetic parameters details)

Table 4 Isoconversional methods used in this work for the kinetic analysis of simulated kinetic curves [3]

Method	Kind	Linear plot equation
Friedman (FR)	Differential	$\ln\left[\left(\frac{\mathrm{d}\alpha}{\mathrm{d}t}\right)_{\alpha}\right] = \ln\left[\beta\left(\frac{\mathrm{d}\alpha}{\mathrm{d}T}\right)_{\alpha}\right] = \ln\left[f(\alpha)A_{\alpha}\right] - \frac{E}{RT_{\alpha}}$
Coats-Redfern (CR)	Integral	$\ln \frac{\beta}{T^2} = \ln \left[\frac{AR}{Eg(\alpha)} \left(1 - \frac{2RT}{E} \right) \right] - \frac{E}{RT}$
Kissinger-Akahira-Sunose (KAS)	Integral	$\ln \frac{\beta}{T^2} = \text{Const.} - \frac{E}{RT}$
Flynn-Wall-Ozawa (FWO)	Integral	$\frac{\mathrm{dlog} \beta}{\mathrm{d} 1/T} \cong \frac{0.457}{R} E$



and Coats-Redfern ones. It is important to mention here that in this work we have only used the traditional isoconversional methods because according to the results obtained by Luciano and Svoboda [29], some of these methods lead to similar E-a curves as the numerical method developed by Vyazovkin [13, 14]. For assessing the most accurate isoconversional methods of Table 4, kinetic curves (α -T and dTG-T) constructed for all the reaction mechanisms included in Table 1 with some of the parameters of Table 2 were analyzed. In Fig. 4, the variation of E with α obtained from the different isoconversional methods is displayed as example for various reaction mechanisms: F1 (a), F1 (b), F2 (c), F2 (d), D1 (e), A2 (f), R3 (g) and P2 (h). The corresponding E and lnA values used in the simulation of the kinetic curves are included in each graph. The E- α curves for the mechanisms F0, D3, A3, A4 and R2 mechanisms are given in Fig. S2 of supplementary material. As we can see, except Flynn-Wall-Ozawa method, which clearly leads to the less accurate values, the other isoconversional methods lead to Evalues very close to the used in the simulation of the kinetic

In Fig. 5, the mean relative error of E has been represented for all the reaction mechanism simulated with different activation energies. Clearly the method leading to the highest error is the Flynn-Wall-Ozawa; however, it is interesting to note that this error increases as activation energy decreases. On the other hand it is also clear that the most accurate results are obtained with the Friedman's, which uses $d\alpha/dT$ values (i.e., dTG-T curves) in the linear plots for estimating the activation energy (see Table 4). For this method, it is also possible to calculate lnA from the intercept of the linear fit performed for each α value. In Fig. 6, InA calculated from the intercept of Friedman method has been plotted for various reaction mechanisms with different Arrhenius parameters (E and lnA). As we can see, lnA values calculated from the intercept are coincident with the corresponding ones used in the simulations of the kinetic curves.

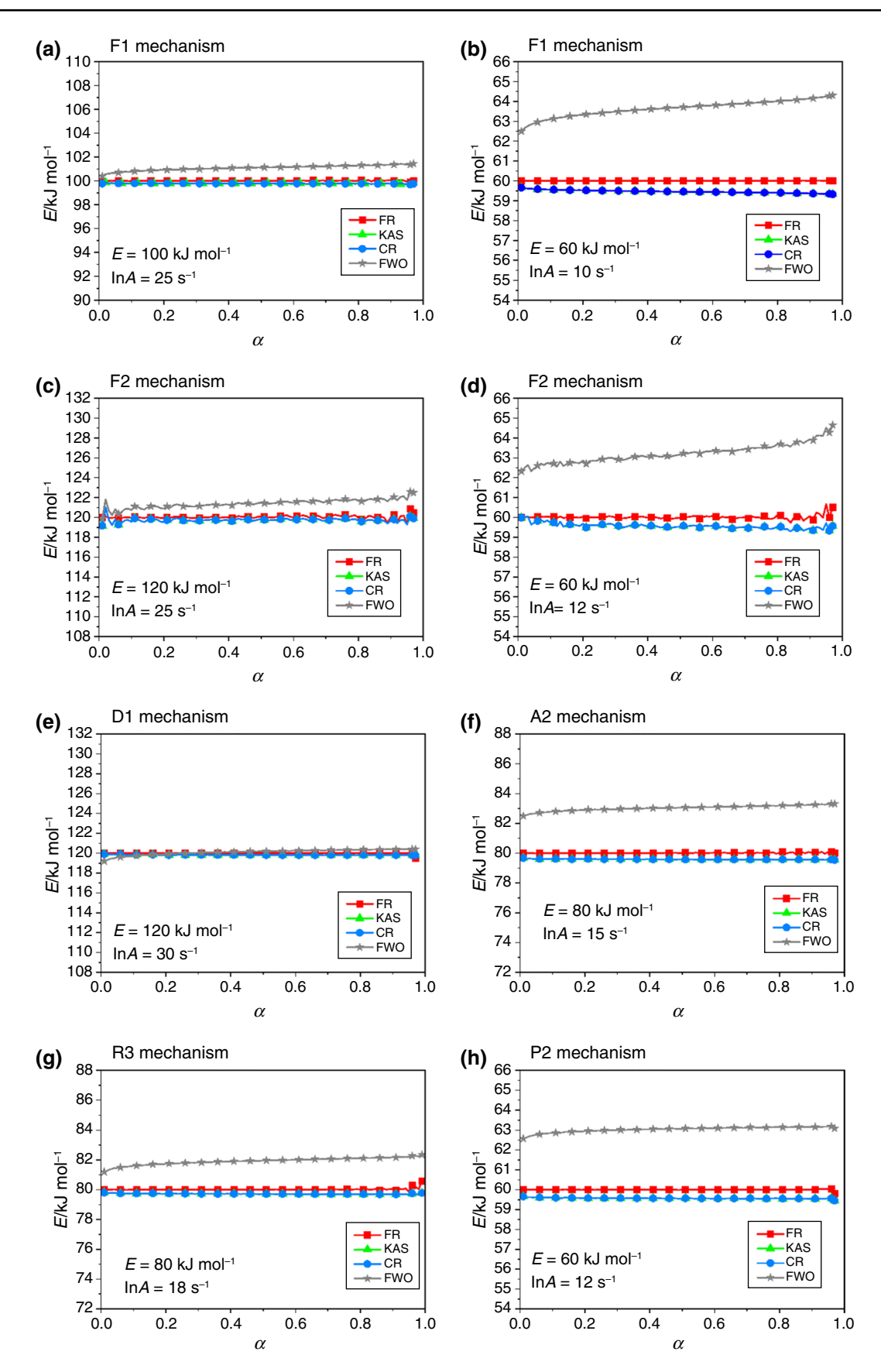
From these results, we can conclude that, although all isoconversional methods lead to activation energy values within an error range quite low (<7%), Friedman method is clearly the most accurate, at least for the case of single-step reaction mechanisms. Actually, being a differential isoconversional method that does not make use of any approximation, it should potentially be more accurate than the integral methods. However, as discussed by Vyazovkin et al. [3] the differential methods should not be considered as being necessary more accurate and precise than the integral ones. In their work, Luciano and Svoboda [29] also mention the relative errors of both KAS and FWO methods. For the first one, they obtained 0,15% while for the second one the error was about 0,8% and hence higher. In our case, relative errors are clearly above the values obtained by Luciano and Svoboda, but this may be due to the fact that our curves were simulated at a much lower points/curve density (100 instead of 10,000) that the E values used by these authors are in the range of 110–300 kJ mol⁻¹ but also that they only simulated F1 and A2 mechanisms. In fact, our calculations for mechanism F1 simulated with E=120 kJ mol⁻¹ showed that relative errors of KAS and FWO methods were 0,228 and 1,06%, respectively, so that very close to the values obtained by Luciano and Svoboda.

Isoconversional analysis was also applied to the multistep reaction mechanisms of Table 3 so that E- α curves were obtained for each method used in this work. The results for all simulated cases (1–7) are displayed in the graphs of Fig. 7a–g with the E values used in the single-step mechanisms included for comparison.

As we can see, for CASES 1 and 2 in which the two mechanisms are clearly differentiated (i.e., peaks in dTG-T curves are slightly overlapping), the transition between the two E values is a well-defined step. This step occurs at the same α value where the step was observed in $(1-\alpha)$ -T curves (see Fig. 2 a), which also corresponds to the contribution of each reaction mechanism to the overall one: CASE 1 with $x_1 = x_2 = 0.5$ and CASE 2 with $x_1 = 0.8$ and $x_2 = 0.2$. As occurred in the analysis of the single-step mechanisms, the curves from FWO method deviate from the E values used in the simulations more than the curves obtained with the other methods, especially when the energy values of the singlestep mechanisms are close (CASES 1, 2, 3 and 7). However, it leads to most accurate activation energy values when those energy values are not very close (CASES 4, 5 and 6). As for FR method, it is interesting to note that it usually produces strong discontinuities (CASES 1, 2 and 6) in the transition interval of E and, in many cases, strong deviations from the activation energy values used in the simulations (CASES 3, 4 and 7). In contrast, KAS and CR methods clearly lead to the most accurate values of activation energies for all simulated cases of multi-step reaction mechanisms, with a smooth and continuous variation of E in the transition interval. It is important to mention that the energy value used for the mechanism R3 (120 kJ mol⁻¹) is only attained in CASE 5, in which the contribution of F2 mechanism is $x_1 = 0.2$ but it is not attained in CASE 4 even for the highest values of conversion when the contribution of F2 mechanism is $x_1 = 0.5$. This must be due to the fact that both mechanisms are highly overlapping, and hence, the one with the lowest energy prevents the one with the highest energy to prevail. Similar results were obtained by Luciano and Svoboda [29] when they compared the results of FR, KAS and FWO methods applied to kinetic curves simulated for multi-step reaction mechanism with different extents of peak overlapping.

From these results, we can conclude that for the case of multi-step reactions, the traditional isoconversional methods are able to give only an estimation of the range of the activation energies associated with the different single-step







∢Fig. 4 Results of FR, KSAS, CR and FWO isoconversional methods for simulated kinetic curves of different reaction mechanisms and Arrhenius parameters. F1 (a), F1 (b), F2 (c), F2 (d), D1 (e), A2 (f), R3 (g) and P2 (h)

mechanisms. Moreover, although Friedman differential method resulted to be the most accurate when analyzing single-step reaction cases, we have seen that the integral methods of Coats-Redfern and Kissinger-Akahira-Sunose lead to better estimations when multi-step reactions are taking place.

Mathematical deconvolution analysis of dTG-T curves

Definition of the peak functions

As discussed above, the use of isoconversional methods in the kinetic analysis of TG measurements is expected to lead to reliable results when single-step reactions occur. However, the most usual situation in real cases is that different processes of decomposition overlap each other so that E varies with α . In general, the overlapping processes are better observed in dTG-T curves (see Fig. 2b) and one of the procedures to separate them is the so-called mathematical deconvolution analysis (MDA). In this kind of analysis, two or more peak curves are used for fitting the experimental dTG-T curves so that single-step reaction mechanisms can be separated and subsequently analyzed. According to the previous experience of different authors [19–22], Fraser-Suzuki (FS) function is very appropriate for deconvoluting curves into single peaks. Most of them have used FS function for deconvoluting either $d\alpha/dt$ -t curves [19, 22] or $d\alpha/dT$ -T curves [20], and in some cases also for deconvoluting heat flow curves [21]. In this work, FS function has been be applied to dTG-T curves so that the general mathematical expression is:

$$\frac{\mathrm{d}\alpha}{\mathrm{d}T} = h\exp\left\{-\frac{\ln 2}{s^2} \left[\ln(1+2s\frac{T-p}{w})\right]^2\right\}$$
 (6)

The four parameters of the function are:

- h: amplitude (peak height)
- s: shape parameter
- p: position
- w: half height width

The main advantage of using $d\alpha/dT$ -T curves in the deconvolution is that their integral along the temperature range should be equal to 1 because, usually, the final

conversion degree of a reaction is $\alpha = 1$, and this applies for both single- and multi-step mechanisms. Therefore, if a $d\alpha/dT$ -T curve is deconvoluted in various curves with a certain contribution, this implies that the integral of each single curve must be equal to 1. Hence, FS curves used in the deconvolution process should meet this requirement, i.e., have a normalized area. According to the authors [17], the area under the Fraser–Suzuki curve is calculated with the following expression, which depends on h, w and s:

$$area = \frac{hw}{2} exp\left(\frac{s^2}{4\ln 2}\right) \left(\frac{\pi}{\ln 2}\right)^{1/2}$$
 (7)

If this area has to be equal to 1, then the parameter *h* can be expressed in terms of the other two:

$$h = \frac{2}{w} \exp\left(-\frac{s^2}{4\ln 2}\right) \left(\frac{\ln 2}{\pi}\right)^{1/2} \tag{8}$$

Therefore, the expression for the normalized Fraser–Suzuki (NFS) function has only 3 parameters: s, p and w.

$$\frac{\mathrm{d}\alpha}{\mathrm{d}T} = \left[\frac{2}{w} \exp\left(-\frac{s^2}{4\ln 2}\right) \left(\frac{\ln 2}{\pi}\right)^{1/2}\right] \exp\left\{-\frac{\ln 2}{s^2} \left[\ln(1+2s\frac{T-p}{w})\right]^2\right\}$$

It is important to note that, in the field of real numbers, the argument of a natural logarithm cannot be zero or negative, so this has to be taken into account in the computing procedure used in $d\alpha/dT$ -T curve deconvolution.

For overcoming this issue, in this work we wanted to check another asymmetric peak function for fitting deconvoluting dTG-T curves. The selected alternative curve is the generalized logistic probability density function (GLOG) [23] whose mathematical expression is:

$$\frac{\mathrm{d}\alpha}{\mathrm{d}T} = \frac{B}{e^{\mathrm{B}(\mathrm{T-T_c})} \left[1 + Qe^{\mathrm{-B}(\mathrm{T-T_c})}\right]^{\left(\frac{1}{\mathrm{Q}} + 1\right)}}$$
(10)

Being a statistic function, it is already normalized so that the area under the curve is equal to 1. GLOG function has three parameters as well: peak position, T_c ; B and Q, while peak height is calculated from the first derivative at T_c as:

$$\frac{\mathrm{d}\alpha}{\mathrm{d}T}\Big|_{T_{c}} = \frac{B}{(1+Q)^{\left(\frac{1}{Q}+1\right)}} \tag{11}$$

It is important to highlight that both NFS a GLOG functions have three parameters, and hence, many combinations could lead to good fitting in a certain MDA procedure. This means that stablishing the range for the initialization parameters and their most appropriate



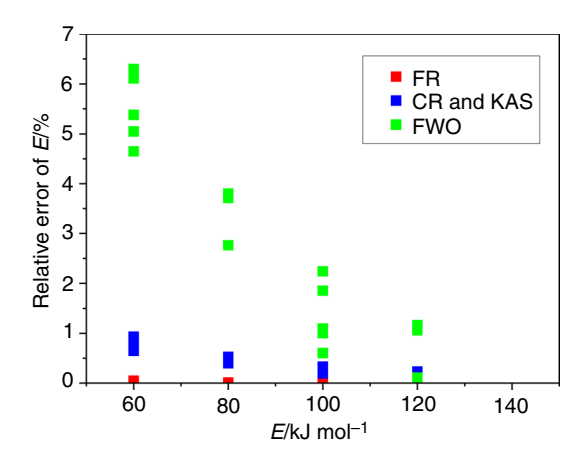


Fig. 5 Relative error of E obtained from the different isoconversional methods

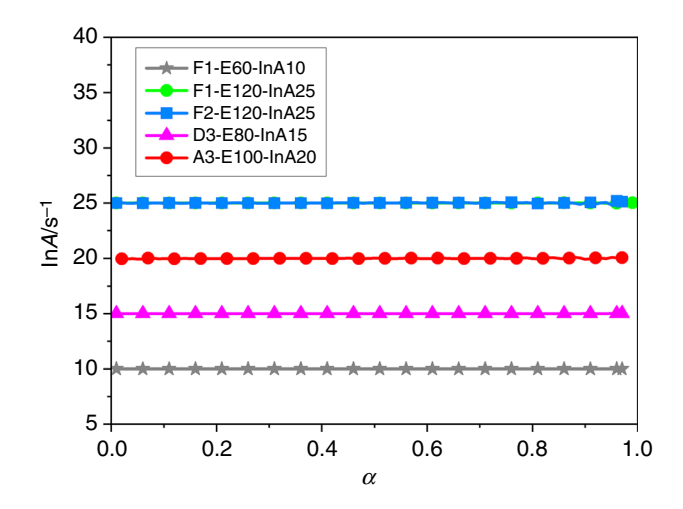
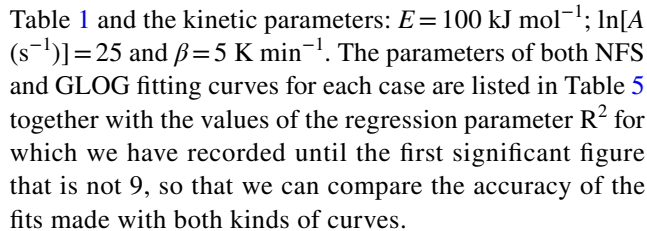


Fig. 6 In A vs. α obtained from the intercept of Friedman method for different simulated mechanisms and Arrhenius parameters

values may be quite difficult if the reaction mechanism is unknown. Therefore, prior to any MDA it would be worth having an estimation of the values taken by the parameters of these functions depending on which reaction mechanism they are representing.

Fitting dTG-T curves of different reaction mechanisms with NFS and GLOG functions

In order to investigate whether these peak functions can properly fit the different reaction mechanisms or which one would be the most appropriate in each case, dTG-T curves simulated by using Eq. 2 were fitted with both NFS and GLOG functions. Curve fitting was done with the "Nonlinear curve fit" tool of Origin 8[©] software by creating generic NFS and GLOG functions. dTG-T curves were simulated for the reaction mechanisms recorded in



For the majority of reaction mechanisms analyzed, fittings with NFS function led to a higher R^2 value so that this curve seems to be more appropriate than GLOG for substituting the kinetic curves in MDA process. Perejón et al. [19] also compared Gaussian, Lorentzian and Fraser–Suzuki functions for fitting dTG-T curves of various reaction mechanisms (F1, R2, R3, A2, A3, A4, D2, D3, D4 and L2). In their study, they came to the conclusion that FS function led to the best fitting results and hence was the most appropriate for deconvoluting experimental dTG-T curves. Cheng et al. [20] also showed that FS function fitted very well the curves of distributed activation energy models (DAEM) for Fn mechanisms with n values from 1 to 2.5, obtaining the best fitting results for the first-order (F1) mechanism. However, our study clearly shows that GLOG function leads to a better dTG-T curve fitting for the reaction models F0, F2 and D1 (see R² column in Table 5). In terms of fitting parameters, peak position (p in NFS and T_c in GLOG) is the one directly associated with the activation energy. Actually, as shown in Table 5, its value remains almost constant not only for all mechanisms but also for both types of fitting curves. However, the other two parameters (w and s for NFS; B and Q for GLOG) strongly vary from one mechanism to another. In Fig. 8a-f, examples of the best curve fittings are displayed. For mechanisms F1, A2, R3 and P2 a-d, NFS fitting is shown while for mechanisms F0 and D1 (e-f) GLOG fitting is the one displayed.

Effect of kinetic parameters in NFS and GLOG parameters

As discussed in previous section, peak position (p in NFS and T_c in GLOG) is the parameter that most clearly depends on the activation energy, E, but in fact if we have a look to the sets of curves plotted in Fig. 1, peak position also varies with the heating rate, β . Therefore, to carry out deconvolutions with kinetic sense it is necessary to find out the possible correlations between the kinetic parameters ($f(\alpha)$, E, InA and β) and the parameters of NFS and GLOG functions, and specially the interval of coherent values.

In this sense, we applied a procedure similar to the one introduced by other authors [20, 21], which consists in simulating dTG-T curves in which all the kinetic parameters are varied within a certain range and then determining their influence in the parameters of NFS and GLOG functions used in the curve fitting. In our case, dTG-T curves



were simulated for all the reaction mechanisms recorded in Table 1 and by varying the kinetic parameters within the following interval: E=60-120 kJ mol⁻¹; lnA[s⁻¹]=12-30; and β =2-20 K min⁻¹. Then we used both NFS and GLOG functions for fitting the simulated curves. For simplifying the discussion, the results have been graphically presented below. The specific values of both simulation and fitting parameters are given in Table S1 of supplementary material.

For the case of dTG-T curves fitted with NFS function, p and w depend on both the kinetic parameters and the heating rate while the shape parameter, s, only depends on the reaction mechanism used in the simulation. In Fig. 9, the variation of both p (a) and w (b) with the heating rate β is plotted as example for the case of dTG-T curves constructed for F1 mechanism and different values of E and E and E and E both parameters decrease as E and E are the same E are the same E are the same E are the same E and E are the same E and E are the same E and E are the same E and E are the same E and E are the same E are the same

When dTG-T curves are fitted with GLOG function, Q is the only parameter depending on the reaction mechanism chosen. However, as happens with NFS function, $T_{\rm c}$ and B depend on the kinetic parameters and heating rate for a given mechanism. In Fig. 10, the variation of both $T_{\rm c}$ (a) and B (b) with heating rate β is plotted as example for the case of dTG-T curves constructed for F0 and D1 mechanisms and different values of E and lnA.

In the case GLOG function, only $T_{\rm c}$ increases with the heating rate while B has a decreasing trend. It is quite obvious that $T_{\rm c}$ in GLOG must follow the same trend as p in NFS because both represent the position of the dTG-T curve maximum. Hence, for the same E, $T_{\rm c}$ is higher for lower $\ln A$, while for the same $\ln A$, $T_{\rm c}$ is higher if E is higher. As for B parameter, it slightly decreases with the heating rate, and for the same E, it has higher values for higher $\ln A$ while for the same $\ln A$, this parameter decreases if E is increased.

Since s and Q parameters are only dependent on the reaction mechanism $f(\alpha)$, the values recorded and highlighted in Table 5 should be used at least as boundary conditions in the whole MDA process. Also it would be important to check which set of s or Q values leads to the best deconvolution results, meaning that each single-step reaction should be represented by a single s or Q value taken from Table 5. In contrast, since the other parameters (p and w for NFS curve; T_c and B for GLOG curve) depend on Arrhenius parameters (E and lnA) and heating rate (β) , their inter-correlation is not as straightforward so that they must remain free in the MDA process. Moreover, we have to take into account that apart from the parameters included in the peak functions, each deconvolution requires a contribution coefficient for each single-step mechanism included in the overall dTG-T curve, which may not be the same for all the heating rates. This would increase even more the number of possibilities in the MDA fitting parameters and make it more complicated.

Deconvolution of simulated dTG-T curves for multi-step reaction mechanisms

In this section, MDA process was applied to the dTG-T curves of the multi-step reaction mechanisms recorded in Table 3. In all cases, either NFS or GLOG functions were used in order to see whether the single-step mechanisms used in the construction could be easily separated and subsequently analyzed. In Fig. 11, the deconvolutions for dTG-T curves simulated with $\beta = 2 \text{ K min}^{-1}$ for CASE 1 (a), CASE 3 (b), CASE 4 (c) and CASE 6 (d) are displayed as example. In all the graphs, the simulated curves are plotted with the deconvoluted single-step mechanism curves and the total curve. As we can see, the curves resulting from deconvolution fit quite well the simulated curves. The parameters of the single-step curves for each case are given in Table S2 (NFS) and Table S3 (GLOG) of supplementary material. The residuals of the deconvolutions displayed in Fig. 11 are shown in Fig. S3 also included in the supplementary material.

Kinetic analysis of deconvoluted curves

Once dTG-T curves of multi-step reaction mechanisms have been deconvoluted and single-step mechanisms separated, different approaches can be applied for obtaining the corresponding kinetic triplets. Activation energy, E, can be calculated by applying some of the isoconversional methods discussed in Sect. "Model-free isoconversional methods for the analysis of single- and multi-step reaction mechanisms." In such case, the resulting E should be a constant value independent of α . However, if a single-step mechanism is assumed, E could be also calculated by the Kissinger method [21] derived from Eq. 1 under the condition of maximum reaction rate [11], which implies that $d^2\alpha/d^2t=0$ leading to the equation:

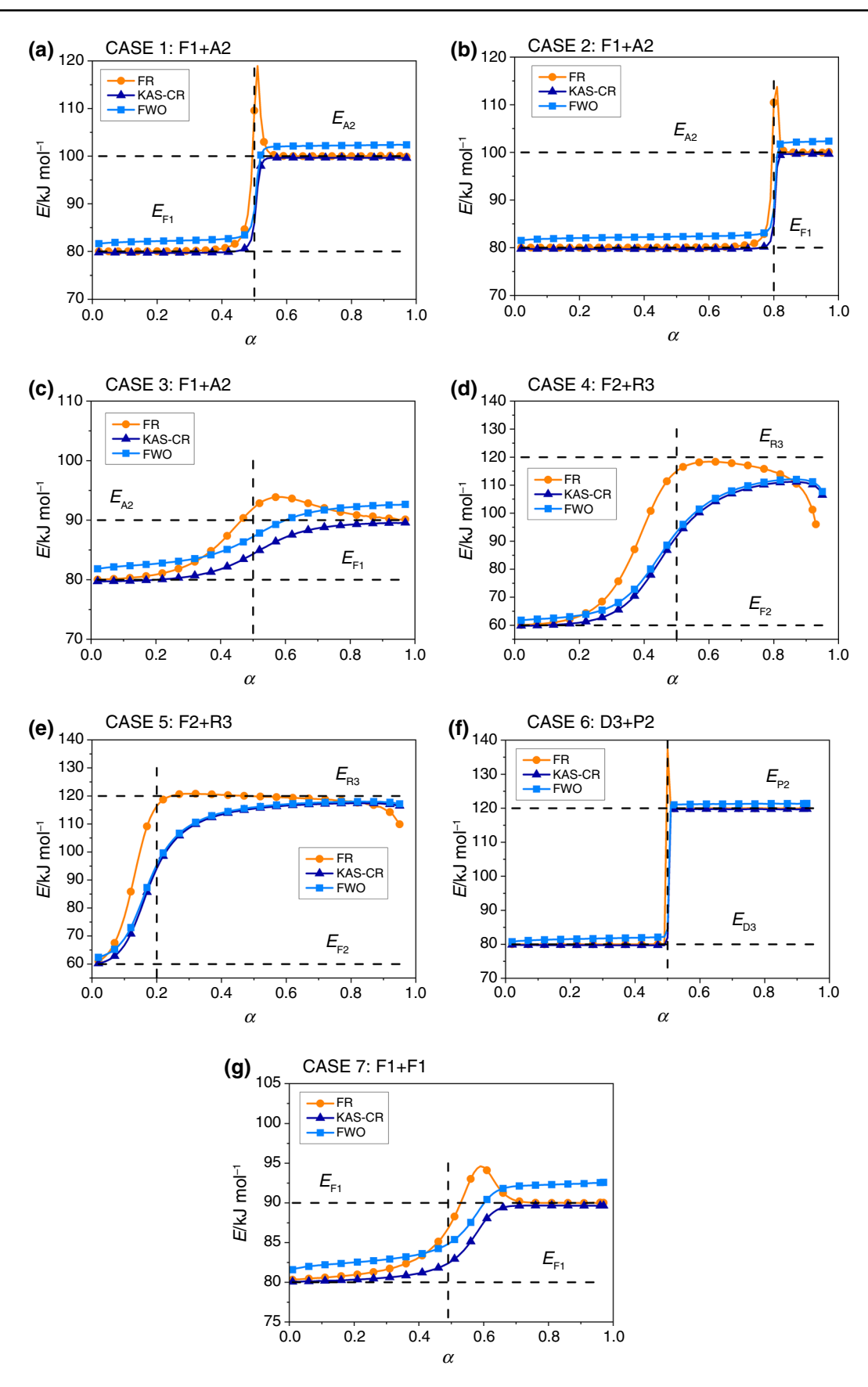
$$\frac{E\beta}{RT_{\rm m}^2} = -Af'(\alpha)e^{\left(\frac{-E}{RT_{\rm m}}\right)}$$
 (12)

where $T_{\rm m}$ corresponds to the temperature at which maximum reaction rate occurs, i.e., where dTG-T curve maximum is located. After a simple rearrangement, Eq. 12 is transformed in:

$$\ln\left(\frac{\beta}{T_{\rm m}^2}\right) = \ln\left[-\frac{AR}{E}f'(\alpha_{\rm m})\right] - \frac{E}{RT_{\rm m}} \tag{13}$$

Hence, by plotting $\ln\left(\frac{\beta}{T_{\rm m}^2}\right)vs.\frac{1}{T_{\rm m}}$, E is obtained from the slope of the linear fitting. We applied this method to the single-step reaction sets of curves obtained in Sect. "Deconvolution of simulated dTG-T curves for multi-step reaction







<Fig. 7 E-α curves calculated for kinetic curves multi-step reaction mechanisms of CASE 1 (a), CASE 2 (b), CASE 3 (c), CASE 4 (d), CASE 5 (e), CASE 6 (f) and CASE 7 (g)

mechanisms" from MDA performed with both NFS and GLOG functions. For the case of NFS curves, $T_{\rm m}$ corresponds to the parameter p, whereas for the GLOG curves, $T_{\rm m}$ corresponds to the $T_{\rm c}$ parameter. In Table 6, E values calculated from the linear fittings of Eq. 13 are recorded for each simulated case together with the relative error. In general, we can say that calculated E values are very close to the ones used in the curve simulations not only for the case of the NFS functions but also for the GLOG functions. Actually, both fittings lead to similar errors in terms of accuracy of E.

For calculating the pre-exponential factor and determining the reaction mechanism, several approaches can be applied as well. One of them is the so-called combined kinetic analysis [19, 34], which allows obtaining the kinetic triplet by using a general expression for $f(\alpha)$. Another method is the one based on master plots of two special functions: $y(\alpha) = Af(\alpha)$ and $z(\alpha) = f(\alpha)g(\alpha)$ [3, 35]. However, according to Eq. 12, it should also be possible to obtain the pre-exponential factor lnA and the reaction mechanism $f(\alpha)$ from the intercept of the linear fitting and this is the method we have used in this work because we already know the single-step reaction mechanisms and we wanted to check the validity of Kissinger method. For that purpose, α -T curve has to be calculated by numerically integrating the fitted curves so that the values of $\alpha_{\rm m}$ at $T_{\rm m}$ can be selected and then used for calculating $f'(\alpha_m)$ for the different heating rates. In principle, $\alpha_{\rm m}$ should remain constant for all rates and so should be $f'(\alpha_m)$. The mathematical expressions of $f'(\alpha)$ for the reaction mechanisms of Table 1 are recorded in Table S4 of supplementary material. The calculations were performed only for some cases so that the validity for different reaction mechanisms could be checked (see Table 6). Apparently, the lnA values calculated from the intercept seem to be quite close to the values used in the simulations of the different multi-step reaction mechanisms not only for MDA performed with NFS but also with GLOG functions. However, since these are logarithmic values the relative error of this parameter is in some cases very high, especially if the mechanisms have dTG-T curves highly asymmetric. To our opinion these errors could be due to the fact that the peak functions used in MDA are only able to reproduce with highly accuracy reaction mechanisms with highly symmetric dTG-T curves [19, 20]. In those cases, the value of $\alpha_{\rm m}$ (and $f'(\alpha_m)$,) obtained from the numerical integration of the peak functions may have some deviations that strongly affect the calculation of lnA from the intercept of Kissinger method. However, if we take into account that other authors have mainly used F1 mechanism for simulating and deconvoluting dTG-T curves of multi-step reactions [19–22], our results extend the validity of using either NFS or GLOG functions for MDA of dTG-T curves of multi-step reactions composed by single-step reaction mechanisms other than F1. In any case, it has to be assumed that the less symmetrical the dTG-T curves are, the less accurate is the MDA procedure either using NFS or GLOG function. This means that other methods should be applied as well for the kinetic analysis of TG measurements where multi-step reaction mechanisms are taking place.

Application to experimental TG measurements of polymeric PCM

The theoretical background introduced in previous sections for simulated kinetic curves was applied to the case of TG measurements taken for polyethylene glycol (PEG) with two molecular sizes: PEG3000 and PEG12000 with the aim of having a preliminary kinetic analysis of the thermal degradation of this PCM. For this purpose, TG measurements were taken under N_2 and air atmospheres (50 mL min⁻¹ flow rate) at heating rates 2, 5, 10 and 20 K min⁻¹ in a XTAR 6000 TG apparatus. TG measurements also provided differential thermal analysis (dTA) signal from which melting temperature was estimated since the apparatus was calibrated in terms of heat flow with metallic indium as reference material. Both polymers PEG3000 and 12000 led to similar onset melting temperatures in the range 53-56 °C for the measurements taken under both air and N₂ atmospheres. These values are in agreement with the values obtained by other authors for this polymeric PCM [26–28].

In Fig. 12, dTG-T curves of PEG12000 are displayed for all the heating rates used in the TG runs performed under air (a) and N_2 (b). Strong differences are observed in the polymer behavior depending on the flowing gas used in the measurements. This indicates that the degradation reactions depend on the surrounding atmosphere. It is important to mention that PEG3000 showed quite the same thermal behavior as PEG12000 leading to dTG-T curves with similar shapes and temperature positions for the different heating rates. The curves of PEG3000 are shown in Fig. S4 of supplementary material. From these curves, it is quite clear that the temperature at which maximum degradation rate occurs strongly depends on the heating rate used in the TG experiment and so is the temperature at which PEG degradation is expected to start. This supports the importance of carrying out a kinetic analysis of the TG measurements that requires tests at various heating rates [24–28].



Table 5 Parameters of NFS and GLOG functions associated with different reaction mechanisms $f(\alpha)$

	NFS fit				GLOG fit			
Model	p/K	S	w/K	\mathbb{R}^2	T _c /K	B/K^{-1}	Q	\mathbb{R}^2
F0	398.6	-1.33	6.9	0.98	399.5	4.263	52.00	0.997
F1	400.0	-0.32	30.8	0.99995	400.0	0.172	2.40	0.996
F2	399.2	0.095	47.6	0.997	399.4	0.074	0.75	0.99991
D1	396.7	-1.34	13.3	0.97	399.3	4.156	100.00	0.997
D3	372.9	-0.49	41.8	0.998	373.1	0.152	3.20	0.990
P2	399.4	-1.23	4.1	0.990	399.3	2.561	16.00	0.97
A2	400.6	-0.36	15.3	0.99994	400.6	0.357	2.60	0.996
A3	400.7	-0.38	10.1	0.99993	400.7	0.535	2.60	0.996
A4	400.8	-0.38	7.6	0.99992	400.7	0.712	2.60	0.996
R2	391.5	-0.68	18.7	0.997	391.9	0.428	6.00	0.990
R3	386.8	-0.55	21.9	0.9990	387.2	0.321	4.50	0.991

Calculation of E-α curves

The isoconversional methods discussed in Sect. "Modelfree isoconversional methods for the analysis of singleand multi-step reaction mechanisms" were applied to the sets of experimental TG measurements of PEG3000 and PEG12000 and the resulting E- α curves are displayed in Fig. 13. Strong differences are observed between the curves obtained for the TG measurements under N₂ (Fig. 13 a, c) and under air (Fig. 13 b, d), with both PCMs showing a similar behavior. For the case of TG measurements under N_2 , Egoes from values around 40 kJ mol⁻¹ at low conversions up to 150 kJ mol⁻¹ at high conversions. Moreover, important differences are observed between the E- α curve obtained by FR method and the curves obtained with KAS-CR and FWO methods. However, this behavior also happened when the simulated multi-step mechanisms were analyzed with the isoconversional methods (see Fig. 7), especially when the single-step mechanisms were highly overlapping. This means again that FR method might not be the most appropriate for predicting E values when multi-step reaction mechanisms occur. The isoconversional analysis of TG measurements under air flow leads to a more constant value of E with α for both PCMs. For PEG3000 this value is 50 ± 12 kJ mol⁻¹ while PEG12000 shows a stronger variation range that goes from 75 to 50 kJ mol⁻¹. Again the results of FR method rather deviate from the results of the other isoconversional methods. The fact that the E values obtained for the TG experiments performed under air clearly indicate that the combustion is the main thermal degradation process occurring in this polymer.

Deconvolution of dTG-T curves

In order to have a preliminary estimation of the possible single-step mechanisms occurring in the degradation of these two PCMs, which clearly are not the same under air or nitrogen, dTG-T curves were deconvoluted by using both NFS and GLOG functions. It must be pointed out that this was not a simple task because, as shown in Fig. 12, the behavior of the experimental curves is quite far from the behavior displayed by the curves theoretically simulated (see Fig. 2). Moreover, for more than two single-step reactions, deconvolutions involve many parameters even if some of them may have the restricted values given in Table 5 as was already discussed in Sect. "Fitting dTG-T curves of different reaction mechanisms with NFS and GLOG functions." In Fig. 14, some deconvolution examples of dTG-T curves of PEG12000 by using NFS functions are displayed. In principle, it seems that quite good deconvolutions can be achieved with either 3 or 2 NFS functions. Similar results were obtained for dTG-T curves of PEG3000.

Kissinger method of Eq. 12 was applied to the deconvoluted curves so that E could be estimated for each single-step mechanism. In Table 7, the activation energies obtained for the different sets of deconvoluted curves with NFS functions have been recorded for the measurements under N_2 and air atmospheres of both PCMs.

If we compare E values of Table 7 with the corresponding E- α curves calculated from the isoconversional methods and displayed in Fig. 13, we can see that they are in quite good agreement and quite well correlated, taking into account that these are only preliminary estimations. According to Table 7, for the measurements under N_2 there are two single-step mechanisms: one with much lower activation energy



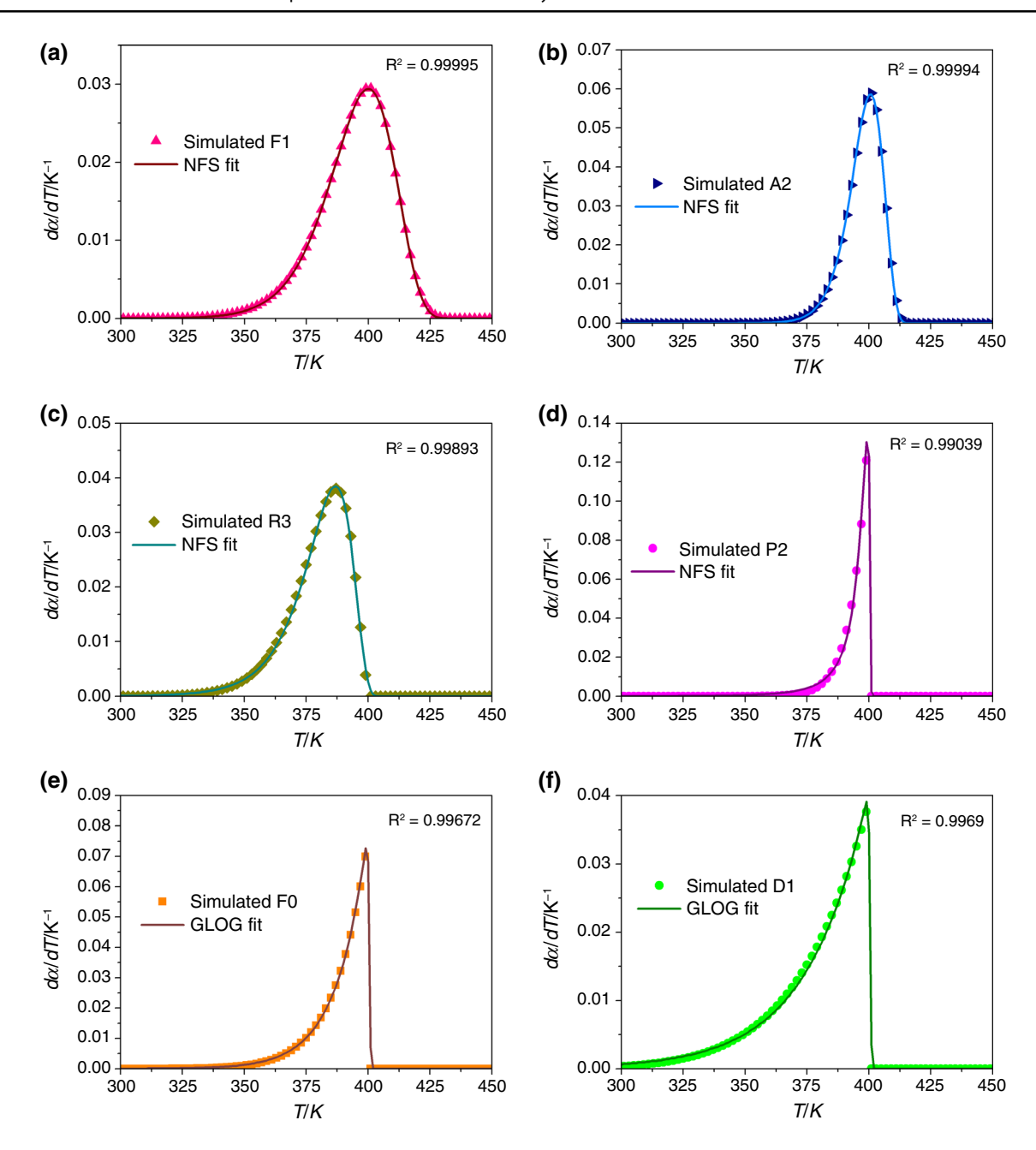


Fig. 8 Examples of dTG-T curves simulated for different reaction mechanisms $f(\alpha)$ and numerical fitted with NFS (a-d) and GLOG functions (d-f)

 $(47-64 \text{ kJ mol}^{-1})$ than the other $(162-196 \text{ kJ mol}^{-1})$. This should lead to strong variation of E with the conversion, as it is observed in the curves of Fig. 13. In contrast, for the measurements under air, the activation energies of the three single-step mechanisms are not that different which leads to only a slight variation of E with α . It is interesting to note that according to the E values obtained, PEG12000 seems to degrade faster than PEG3000 because it has lower values of activation energy specially under nitrogen. However, this conclusion may not be fully correct since the studies found

in the literature for PEG with molecular weights between 1500 and 6000 do not show big differences in terms of TG behavior. Hence, if a correlation wants to be obtained in terms of PEG molecular size, TG measurements and kinetic analyses for other PEG with different molecular weights should be carried out.

As for the determination of the other kinetic parameters lnA and $f(\alpha)$ associated with the single-step mechanisms, they would require the development of the methods of



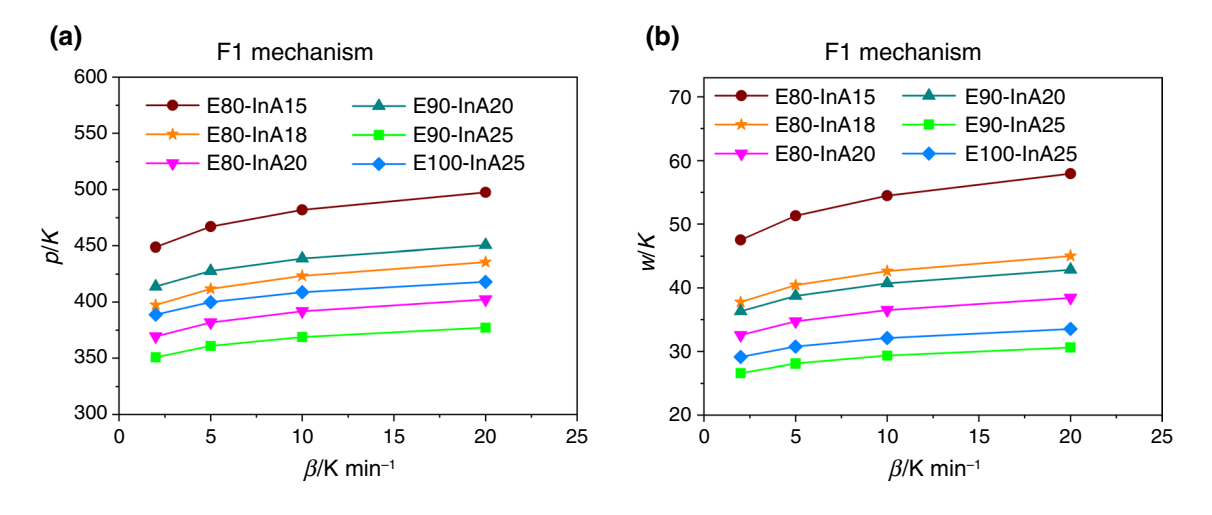


Fig. 9 Variation of NFS parameters (p and w) with β , E and lnA for a reaction mechanism F1

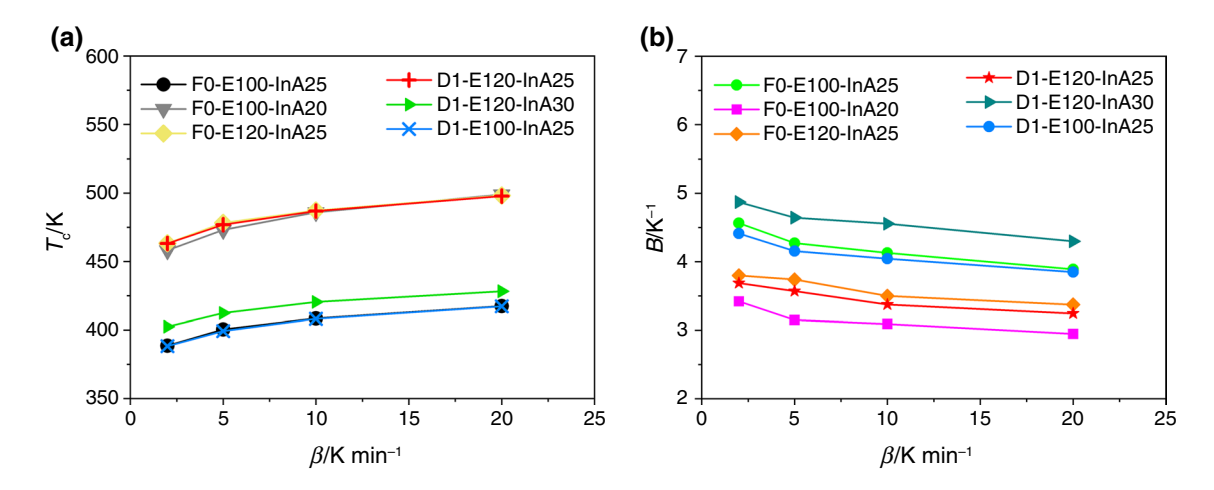


Fig. 10 Variation of GLOG parameters: T_c (left) and B (right) with β and Arrhenius parameters, for reaction mechanisms F0 and D1



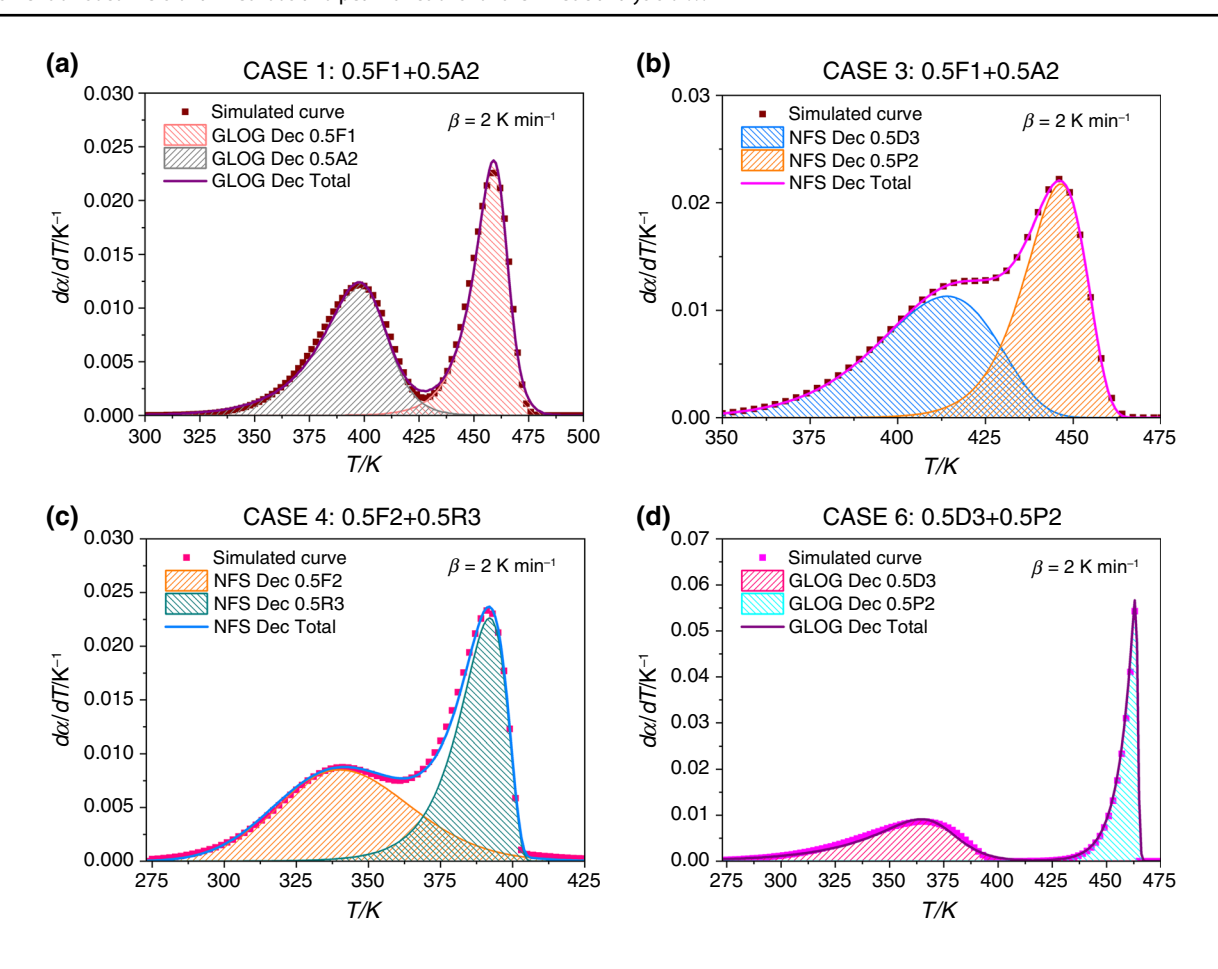


Fig. 11 Deconvolution of dTG-T curves for some simulated multi-step reaction mechanisms: a CASE 1; b CASE 3; c CASE 4; and d CASE 6 (see Table 3)

Table 6 Kinetic parameters obtained with Kissinger method for the multi-step reaction mechanisms simulated and then deconvoluted with both NFS and GLOG functions

					E and lnA from Kissinger method			
			Simulated	NFS			GLOG	
	Mechanism	x	E/kJ mol ^{−1}	lnA/s ⁻¹	E/kJ mol ⁻¹	lnA/s ⁻¹	E/kJ mol ⁻¹	lnA/s ⁻¹
CASE 1	F1	0.5	80	18	79.71 (0.36%)	17.89 (10.4%)	79.90 (0.13%)	17.97 (2.9%)
	A2	0.5	100	20	99.73 (0.27%)	20.02 (22.14%)	99.63 (0.37%)	19.94 (5.8%)
CASE 2	F1	0.8	80	17	78.50 (1.87%)		79.76 (0.30%)	
	A2	0.2	100	20	100.39 (0.39%)		99.45 (0.55%)	
CASE 3	F1	0.5	80	17	79.58 (0.53)%		79.07 (1.16%)	
	A2	0.5	90	18	89.54 (0.51%)		89.89 (0.12%)	
CASE 4	F2	0.5	60	15	59.57 (0.72%)	14.81 (17.3%)	57.52 (4.13%)	
	R3	0.5	120	30	120.30 (0.25%)	32.76 (1479%)	119.96 (0.03%)	
CASE 6	D3	0.5	80	18	78.47	17.43 (43.4%)	79.11	17.63 (30.9%)
	P2	0.5	120	25	119.46	24.81 (17.3%)	119.24	24.74 (22.9%)
CASE 7	F1	0.5	80	19	79.97 (0.04%)		79.04 (1.2%)	
	F1	0.5	90	19	89.93 (0.08%)		89.30 (0.08%)	



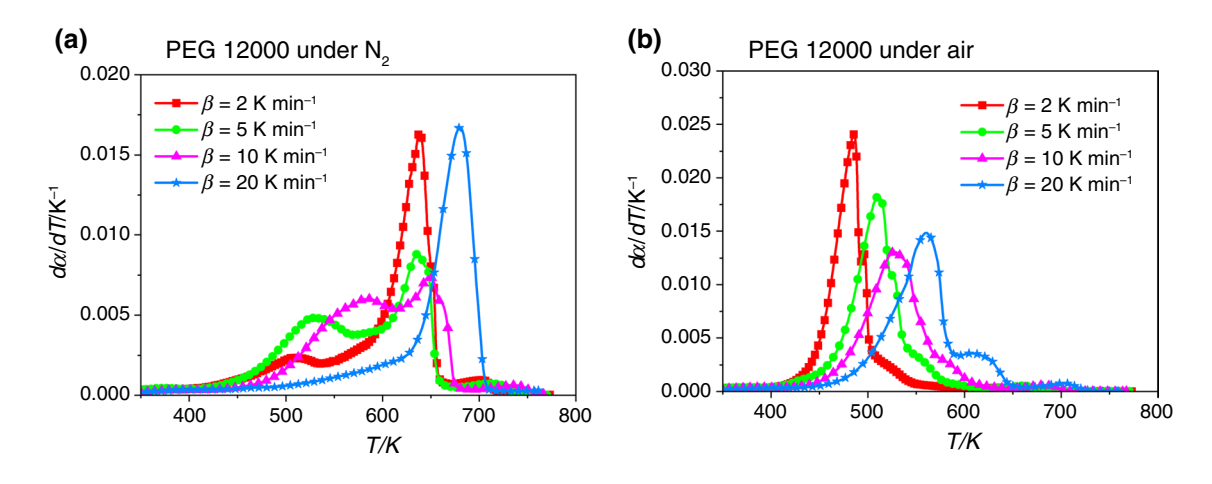


Fig. 12 dTG-T curves of PEG 12000 obtained at different heating rates under air (a) and N₂ (b) atmospheres

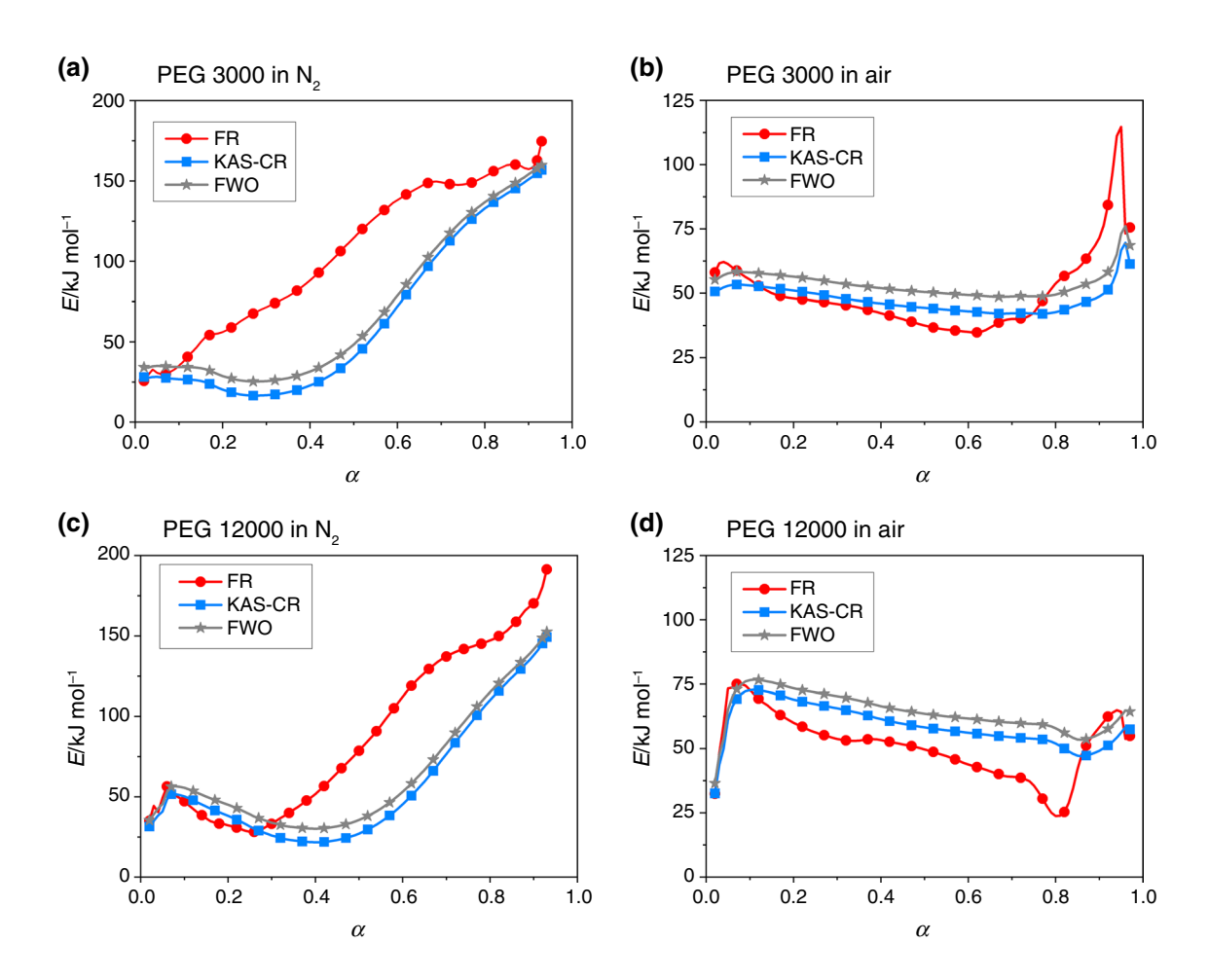


Fig. 13 E vs. α curves of PEG3000 and PEG12000 for TG measurements taken under N_2 and air obtained from the isoconversional methods used in this work



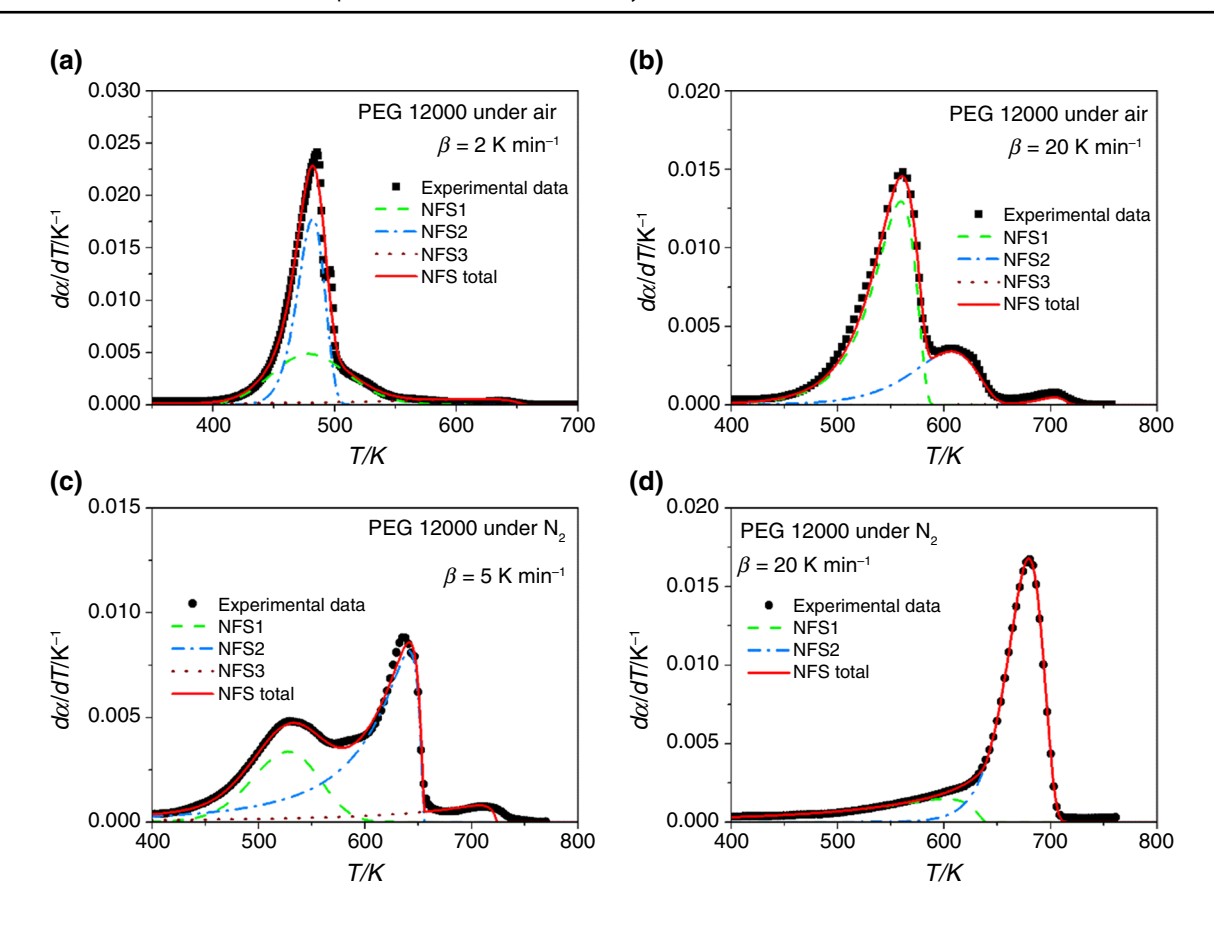


Fig. 14 Examples of dTG curves deconvolutions using NFS functions for PEG12000 at different heating rates and TG measurements under air and N_2 atmospheres

 Table 7
 Estimated E for deconvoluted peaks obtained with NFS functions

		E from Kissinger method/kJ mol ⁻¹				
	Atmosphere	Curve 1	Curve 2	Curve 3		
PEG 3000	$\overline{N_2}$	64	196	_		
	Air	50	40	93		
PEG 12000	N_2	47	162	_		
	Air	57	37	93		

combined kinetic analysis and master plots, which for the moment are beyond the scope of this paper.

Conclusions

In this work, theoretical kinetic curves α -T and dTG-T were simulated for both single-step and multi-step reaction mechanisms by using different sets of kinetic triplets ($f(\alpha)$, E and $\ln A$). These curves were analyzed with various isoconversional methods so that E- α curves were obtained and compared with the energy values used in the simulations. For the

single-step reaction mechanisms, all methods lead to activation energies within an error range below 7% in relation to the values used in the simulations, being Friedman method the most accurate. For the multi-step reaction mechanisms, the obtained E- α curves were only a rough estimation of the activation energies used in the simulations and, in this case, Kissinger–Akahira–Sunose and Coats–Redfern methods were the ones leading to the most accurate results.

Simulated dTG-T curves of single-step mechanisms were fitted with two kinds of peak functions (normalized Fraser–Suzuki—NFS and generalized logistic—GLOG) in order to determine which one better represented the different reaction mechanisms. Although both functions led to regression values above 0,99, the NFS proved to better fit dTG-T curves of the majority of reaction mechanisms analyzed. From the fitting, the relationship between the kinetic triplet used for simulating dTG-T curves and the parameters of NFS and GLOG functions was obtained as well. Both functions had only one parameters that depended on the reaction mechanism used in the simulation (s for NFS; Q for GLOG) while the other two depended on both the Arrhenius parameters, E and lnA, and the heating rate, β (p and p for NFS; p and p for GLOG). These relationships



will be strongly helpful when experimental dTG-T curves of multi-step reactions have to be analyzed by applying mathematical deconvolution analysis (MDA). In this sense, the values of s and Q parameters associated with the different reaction mechanisms should be used as boundary conditions. Moreover, to the author knowledge this is the first time both normalized Fraser–Suzuki and generalized logistic functions have been used for fitting dTG-T curves of different reaction mechanisms.

MDA was applied to dTG-T curves of multi-step reaction mechanisms by using both NFS and GLOG functions and taking into account the relationships between the kinetic triplet and the function parameters obtained in this work. With this procedure, single-step reaction peaks were separated and their corresponding kinetic parameters calculated. In general, the curves resulting from deconvolution fitted quite well the simulated curves and the analysis of the single-step peaks with Kissinger method leads kinetic triplets quite close to the ones used in the simulations mainly for single-step mechanism with dTG-T curves with high symmetry. Compared with similar studies found in the literature, which are mostly focused in reaction mechanism F1, our results extend the validity of using either NFS or GLOG functions for deconvoluting dTG curves composed by many other reaction mechanisms. However, it must be taken into account that deconvolution of experimental dTG-T curves may be complicated if single-step reaction mechanisms are strongly overlapped and their contribution to the overall reaction varies with the conversion.

A similar procedure of kinetic analysis was applied to thermogravimetric measurements taken under both air and N_2 atmospheres for two PCMs: PEG3000 and PEG12000. In first stage E- α curves were obtained for the different isoconversional methods used in this work. The curves from the measurements under N_2 showed E values going from around 40 kJ mol⁻¹ at low conversions up to 150 kJ mol⁻¹ at high conversions, whereas the curves from TG measurements under air showed more constant E values of about 50–75 kJ mol⁻¹. The lower activation energies obtained for the measurements under air are most probably an indication of the polymer combustion.

Finally, experimental dTG-T curves were deconvoluted with the most appropriate peak functions in order to have a preliminary estimation of the possible single-step reaction mechanisms occurring in these PCMs. For both PEG, fairly good deconvolutions were achieved with either 3 or 2 NFS functions and the resulting single-step reaction curves were analyzed with the Kissinger method. The activation energies obtained from Kissinger method were in good agreement with the $E-\alpha$ curves calculated with the isoconversional methods. As for the other kinetic parameters associated with the single-step mechanisms, they

would require a further kinetic analysis, which is beyond the scope of this paper.

Supplementary Information The online version contains supplementary material available at https://doi.org/10.1007/s10973-024-13494-w.

Acknowledgements This work has been supported by Comunidad de Madrid and European Structural Funds through ACES2030 Project (S2018/EM-4319), the European Union's Horizon H2020 Research and Innovation Programme through StoRIES Project (GA N° 101036910) and SFERA III Project (GA N° 823802) and also by the STES4D-mat project, Grant TED2021-131061B-C33 funded by MCIN/AEI/https://doi.org/10.13039/501100011033 and by the "European Union NextGenerationEU/PRTR."

Author contributions Rocío Bayón and Redlich García-Rojas were involved in conceptualization, methodology, formal analysis and investigation; Rocío Bayón took part in writing-original draft preparation; Rocío Bayón, Redlich García-Rojas, Esther Rojas and Margarita M. Rodríguez-García participated in writing-reviewing and editing; and Rocío Bayón, Esther Rojas and Margarita M. Rodríguez-García were responsible for funding acquisition and resources.

Funding Open Access funding provided thanks to the CRUE-CSIC agreement with Springer Nature.

Open Access This article is licensed under a Creative Commons Attribution 4.0 International License, which permits use, sharing, adaptation, distribution and reproduction in any medium or format, as long as you give appropriate credit to the original author(s) and the source, provide a link to the Creative Commons licence, and indicate if changes were made. The images or other third party material in this article are included in the article's Creative Commons licence, unless indicated otherwise in a credit line to the material. If material is not included in the article's Creative Commons licence and your intended use is not permitted by statutory regulation or exceeds the permitted use, you will need to obtain permission directly from the copyright holder. To view a copy of this licence, visit http://creativecommons.org/licenses/by/4.0/.

References

- Bayón R, Rojas E. Development of a new methodology for validating thermal storage media: application to phase change materials. Int J Energy Res. 2019. https://doi.org/10.1002/er.4589.
- Bayón R, Bonanos A, Rojas E. Assessing the long-term stability of fatty acids for latent heat storage by studying their thermal degradation kinetics. Proceedings Eurosun. 2020; https://doi.org/ 10.18086/eurosun.2020.07.10
- Vyazovkin S, Burnham AK, Criado JM, Pérez-Maqueda LA, Popescu C, Sbirrazzouli N. ICTAC kinetics committee recommendations for performing kinetic computations on thermal analysis data. Thermochim Acta. 2011. https://doi.org/10.1016/j.tca.2011. 03.034
- Doyle CD. Kinetic analysis of thermogravimetric data. J Appl Polym Sci. 1961. https://doi.org/10.1002/app.1961.070051506.
- Órfão J. Review and evaluation of the approximations to the temperature integral. AICHE J. 2007. https://doi.org/10.1002/aic. 11296.
- Coats W, Redfern JP. Kinetic parameters from thermogravimetric data. Nature. 1964. https://doi.org/10.1038/201068a0.



- Friedman HI. Kinetics of thermal degradation of char-forming plastics from thermogravimetry. Application to a phenolic plastic. J Polym Sci Part C. 1964;6:183–95. https://doi.org/10.1002/polc. 5070060121.
- Ozawa T. A new method for analyzing thermogravimetric data. Bull Chem Soc Japan. 1965. https://doi.org/10.1246/bcsj.38.1881.
- Flynn JH, Wall LA. A quick, direct method for the determination of activation energy from thermogravimetric data. Polymer letters. 1966. https://doi.org/10.1002/pol.1966.110040504.
- Akahira T, Sunose T. Method of determining activation deterioration constant of electrical insulating materials. Res Report Chiba Inst Technol (Sci Technol). 1971;16:22–31.
- Kissinger HE. Reaction kinetics in differential thermal analysis. Anal Chem. 1957. https://doi.org/10.1021/ac60131a045.
- Miura K, Maki T. A simple method for estimating f(E) and k0(E) in the distributed activation energy model. Energy Fuels. 1998. https://doi.org/10.1021/ef970212q.
- Vyazovkin S. Evaluation of the activation energy of thermally stimulated solid state reactions under an arbitrary variation of the temperature. J Comput Chem. 1997. https://doi.org/10.1002/ (SICI)1096-987X(199702)18:3%3c393::AID-JCC9%3e3.0. CO;2-P.
- Vyazovkin S. Modification of the integral isoconversional method to account for variation in the activation energy. J Comput Chem. 2001;22(2):178–83.
- Vyazovkin S, Burnham AK, Favergeon L, Koga N, Moukhina E, Pérez-Maqueda LA, Sbirrazzouli N. ICTAC kinetics committee recommendations for analysis of multi-step kinetics. Thermochim Acta. 2020. https://doi.org/10.1016/j.tca.2020.178597.
- Pomerantsev AL. Kinetic analysis of non-isothermal solid-state reactions: multi-stage modelling without assumptions in the reaction mechanism. Phys Chem Chem Phys. 2017. https://doi. org/10.1039/C6CP07529K.
- Fraser RDB, Suzuki E. Resolution of overlapping bands: functions for simulating band shapes. Anal Chem. 1969. https://doi.org/10.1021/ac60270a007.
- Rusch PF, Lelieur JP. Analytical moments of skewed gaussian distribution functions. Anal Chem. 1973. https://doi.org/10. 1021/ac60330a060.
- Perejón A, Sánchez-Jiménez PE, Criado JM, Pérez-Maqueda LA. Kinetic Analysis of complex solid-state reactions. A new deconvolution procedure. J Phys Chem. 2011;115(8):1780–91. https://doi.org/10.1021/jp110895z.
- Cheng Z, Wu W, Ji P, Zhou X, Liu R, Cai J. Applicability of Fraser-Suzuki function in kinetic analysis of DAEM processes and lingnocellulosic biomass pyrolysis process. J Therm Anal Calorim. 2015. https://doi.org/10.1007/s10973-014-4215-3.
- Svoboda R, Málek L. Applicatility of Fraser-Suzuki function in kinetic analysis of complex crystallization processes.
 J Therm Anal Calorim. 2013. https://doi.org/10.1007/s10973-012-2445-9.
- Stankovic B, Jovanovic J, Adnadjevic B. Application of the Suzuki-Fraser function in modelling the non-isothermal dihydroxylation kinetics of fullerol. React Kinet Mech Cat. 2018. https://doi.org/10.1007/s11144-018-1380-6.

- Richards FJ. A Flexible growth function for empirical use. J Experimental Botany. 1959; https://www.jstor.org/stable/23686 557
- Sheng M, Sheng Y, Wu H, Liu Z, Li Y, Xiao Y, Lu X, Qu J. Bio-based poly (lactic acid) shaped wood-plastic phase change composites for thermal energy storage featuring favorable reprocessability and mechanical properties. Sol Energy Mater and Sol Cells. 2023. https://doi.org/10.1016/j.solmat.2023.112186.
- Chen X, Guo X, Lin X, et al. pH-responsive wood-based phase change material for thermal energy storage building material application. J Mater Sci. 2022. https://doi.org/10.1007/ s10853-022-07474-4.
- Yan D, Zhao S, Ge C, Gao J, Gu C, Fan Y. PBT/adipic acid modified PEG solid-solid phase change composites. J Energy Storage. 2022. https://doi.org/10.1016/j.est.2022.104753.
- Wang Z, Zhang X, Jia S, et al. Influences of dynamic impregnating on morphologies and thermal properties of polyethylene glycol-based composite as shape-stabilized PCMs. J Therm Anal Calorim. 2017. https://doi.org/10.1007/s10973-016-5958-9.
- Liu Z, Zhang Y, Hu K, Xiao Y, Wang J, Zhou C, Lei J. Preparation and properties of polyethylene glycol based semi-interpenetrating polymer network as novel form-stable phase change materials for thermal energy storage. Energy Build. 2016. https://doi.org/10.1016/j.enbuild.2016.06.009.
- Luciano G, Svoboda R. Activation energy determination in case of independent complex 2 kinetic processes. Processes. 2019;7(10):738. https://doi.org/10.3390/pr7100738.
- Muravyev NV, Pivkina AN, Koga N. Critical appraisal of kinetic calculation methods applied to overlapping multistep reactions. Molecules. 2019. https://doi.org/10.3390/molecules24122298.
- Granado L, Sbirrazzouli N. Isoconversional computations for nonisothermal kinetic predictions. Thermochim Acta. 2021. https:// doi.org/10.1016/j.tca.2020.178859.
- 32. Sbirrazzouli N. Model-free isothermal and nonisothermal predictios using advanced isoconversional methods. Thermochim Acta. 2021. https://doi.org/10.1016/j.tca.2020.178855.
- Bayón R, García RJ, Quant L, Rojas E. Study of thermal degradation of adipic acid as PCM under stress conditions: a kinetic analysis. Eurosun Proceedings. 2022; https://doi.org/10.18086/eurosun.2022.13.02
- Pérez-Maqueda LA, Criado JM, Sánchez-Jiménez PE. Combined kinetic analysis of solid-state reactions: a powerful tool for the simultaneous determination of kinetic parameters and the kinetic model without previous assumptions on the reaction mechanism. J Phys Chem A. 2006. https://doi.org/10.1021/jp064792g.
- 35. Málek J. The kinetic analysis of non-isothermal data. Thermochim Acta. 1992. https://doi.org/10.1016/0040-6031(92)85118-F.

Publisher's Note Springer Nature remains neutral with regard to jurisdictional claims in published maps and institutional affiliations.

